To which side are the scales swinging? Growth stability of Siberian larch under permanent moisture deficit with periodic droughts

Dina F. Zhirnova[a], Elena A. Babushkina[a], Liliana V. Belokopytova[a *], Eugene A. Vaganov[b c d]

[a] *Khakass Technical Institute, Siberian Federal University, 27 Shchetinkina, 655017, Abakan, Russia*

[b] *Siberian Federal University, 79 Svobodny, 660041, Krasnoyarsk, Russia*

[c] *Sukachev Institute of Forest, Siberian Branch of the Russian Academy of Sciences, 50/28 Akademgorodok, 660036, Krasnoyarsk, Russia*

[d] *Center for Forest Ecology and Productivity, Russian Academy of Sciences, 84/32 bldg. 14 Profsoyuznaya st., 117997, Moscow, Russia*

[*] Corresponding author: white_lili@mail.ru

Abstract

In moisture-limited regions in which droughts leave a significant "footprint", monitoring of quantitative climatic parameters and of forest adaptation and acclimation to these parameters is of utmost importance due to the ambiguity of spatial patterns in reaction of tree growth to drought and the variety of drought resistance strategies exhibited by trees at the genetic, morphological and physiological levels. This is a case study of the radial growth of Siberian larch (*Larix sibirica* Ledeb.) along the forest-steppe transect in the foothills of the Bateni Ridge (Kuznetsk Alatau, Southern Siberia, Russia) and of its climatic response and stability under the influence of droughts and contributing factors. In this region, a permanent mild moisture deficit is gradually increasing due to warming of the vegetative season by 0.14–0.19°C per decade; droughts occurred in 1951, 1963-65, 1974-76, and 1999. The forests in the region are represented by pure larch stands in the west and mixed stands of larch with Scots pine and silver birch in the eastern portion of the ridge. The forest-steppe ecotone comprises a significant part of the ridge area, mainly on the southern and southeastern slopes. At 5 sampling sites, dependence of larch growth on precipitation (*P*) and standardized precipitation-evapotranspiration index (*SPEI*) during April–July of the current year and June–September of the previous year and on maximum temperature (*Tmax*) during May–July of the current year and July–September of the previous year was observed. We propose the use of a linear regression model based on the *SPEI* of these seasons as an individualized indicator of climate aridity, which is biologically significant for larch in the study area. An analysis of pointer years showed that precipitation in November (formation of snow cover) also contributes to larch growth. The larch in the study area tolerates moisture deficit, rebounding after the end of stress

exposure. The spatiotemporal patterns of the stability indices revealed that despite the decrease in growth resistance and resilience with drought severity, these characteristics are higher at more arid sites due to trees' acclimation to permanent climate aridity. The findings contribute to a better understanding of the capability of larch to further acclimatize and provide a basis for planning measures for conservation and/or restoration of the region's forests under climate warming; however, to clarify the contributions of factors at the individual and local scales, further investigation of the stability of larch growth at the level of individual trees may be required.

Keywords: radial growth; *Larix sibirica;* Kuznetsk Alatau; forest-steppe; climate–growth relationships; pointer years; drought stress

1 Introduction

Climate forecasts predict an increase in the length and intensity of droughts in many regions (Seager et al., 2007; Dai, 2013). Drought is aggravated by warming, which leads to an increase in potential evapotranspiration and, as a result, water stress in vegetation (Allen et al., 2010, 2015; Williams et al., 2013; Serra-Maluquer et al., 2018). Therefore, spatiotemporal analysis and constant monitoring of quantitative climatic parameters and of plants' (including trees) reaction to them become extremely important for regions experiencing moisture deficit, since the "footprints" of droughts in semiarid regions are often more severe than the effects of other dangerous phenomena (Wilhite, 1993; Yatagai, Yasunari, 1995; Dai et al., 1998; Velisevich and Khutornoy, 2009; Dulamsuren et al., 2013). To facilitate this monitoring, a variety of drought indices that take into account climatic, hydrological, and other characteristics of a territory or ecosystem are often used (WMO and GWP, 2016).

Data on the patterns of woody plants' reaction to droughts under various conditions are quite contradictory. For example, growth reduction trends can be more pronounced in populations growing in more xeric (Pasho et al., 2011; Camarero et al., 2013) or more humid areas (Martínez-Vilalta et al., 2012), and the absence of growth stability dependence on local conditions is also observed (Serra-Maluquer et al., 2018). Trees from regions in which there is permanent moisture deficit may be less susceptible to extreme droughts due to their genetic adaptation to low water availability (Chen et al., 2010;

Anderegg et al. 2015). On the other hand, droughts can have significant long-term effects on plants via ecophysiological memory and morphological changes (Peñuelas et al., 2000; Galiano et al., 2011); this is supported by the delayed tree mortality observed in the most extreme cases (Bigler et al., 2006; McDowell et al., 2010; Anderegg et al., 2013; Cailleret et al. 2017). This effect also determines some intra-specific spatial gradients in the drought response (Martínez-Vilalta et al. 2008; Dorman et al. 2013, 2015; Levesque et al. 2014): in drier habitats, structural and physiological acclimation to a permanent moisture deficit is observed, e.g., a lower ratio of the area of leaves and/or fine roots to sapwood or higher stomata control (Delucia et al. 2000; Martinez-Vilalta et al. 2009). Morphological and physiological differences between species also provide different strategies for coping with drought (Maherali et al., 2004; Engelbrecht et al., 2007; McDowell et al. 2008; Lyu et al., 2017). In general, it is difficult to unambiguously answer the question of how forests will resist and recover from drought stress since their reaction can be influenced by many factors (McDowell et al., 2008; Anderegg and HilleRisLambers, 2016; Clark et al., 2016). However, we can with a high degree of certainty assess the point at which effect of stress, including drought, becomes irreversible and leads to forest dieback.

In mountain forests, the lower forest boundary is most severely affected by moisture deficit. The vulnerability of these ecosystems due to their mosaic topography and microclimate (Barber et al. 2000; Kulagin et al. 2006; Lange et al. 2016; Monnier et al. 2012) may lead to a reduction in forest area under conditions of climate warming and increased drought frequency and intensity. In low mountain systems that have a relatively small range of altitudes and natural zones, the forest-steppe ecotone may occupy a substantial portion of the total forest area. A striking example of such a region is the Bateni ridge, the eastern spur of the Kuznetsk Alatau (Russia, Southern Siberia), which we selected as a study area. The Bateni ridge is surrounded on three sides by arid steppes of the Khakass-Minusinsk depression. The purpose of this case study was to conduct a spatiotemporal analysis of the growth response of Siberian larch (*Larix sibirica* Ledeb.), one of the main tree species in the region, to moisture deficit, including droughts. We assume that the drought tolerance of larch has allowed this species to successfully adapt to the conditions on the ridge, participate in the formation of the lower forest boundary there (cf. Bocharov, Savchuk 2015), and successfully acclimatize to the current rapid regional warming.

2 Materials and Methods

2.1 Study area and sampling sites

The study was conducted in the foothills of the Bateni Ridge, the eastern spur of the Kuznetsk Alatau (Fig. 1a). This ridge is characterized by less variation in elevation (500-1200 m a.s.l.) than occurs in the main part of the Kuznetsk Alatau (up to 2000 m a.s.l.). Most of the ridge area is covered by mixed forest consisting of Siberian larch, Scots pine (*Pinus sylvestris* L.) and silver birch (*Betula pendula* Roth.). On the drier southern and southeastern slopes of the ridge, open-stand forests and free-standing trees are interspersed with steppes. The study area belongs to the state forest fund and consists of territories belonging to the Tuim, Bograd, Ust-Byur and Abakan forestries. The archives of the State Forest Committee of the Republic of Khakassia were used in this work as a source of additional data on forest disturbances over the last three decades.

The regional climate is sharply continental (Alisov 1956; Fig. 1b), showing large seasonal and daily temperature variation (*mean*(*Tmax* – *Tmin*) = 9.5–14°C depending on the month; the temperature difference between July and January is ~38°C), hot summer, and frosty winter lasting from November to March with little snow. The average annual temperature ranges from -1.5 to +0.5°C, and the annual precipitation is 470-560 mm, of which approximately 80% falls during the season of positive temperatures, with a maximum in July. The frost-free period (positive minimum daily temperatures) lasts on average from May to September, the same interval during which the mean daily temperatures exceed +5°C. During this season, significant negative correlations of monthly temperature series with precipitation are observed, as is typical for the region (Bazhenova and Tyumentseva, 2010); the correlation ranges from -0.25 to -0.43 for the mean temperature and from -0.35 to -0.61 for the maximum temperature, whereas the minimum temperature does not correlate with precipitation. As a result, the climate of the vegetative season fluctuates between hot-dry and cool-wet modes, i.e., between extreme conditions and conditions favorable for tree growth.

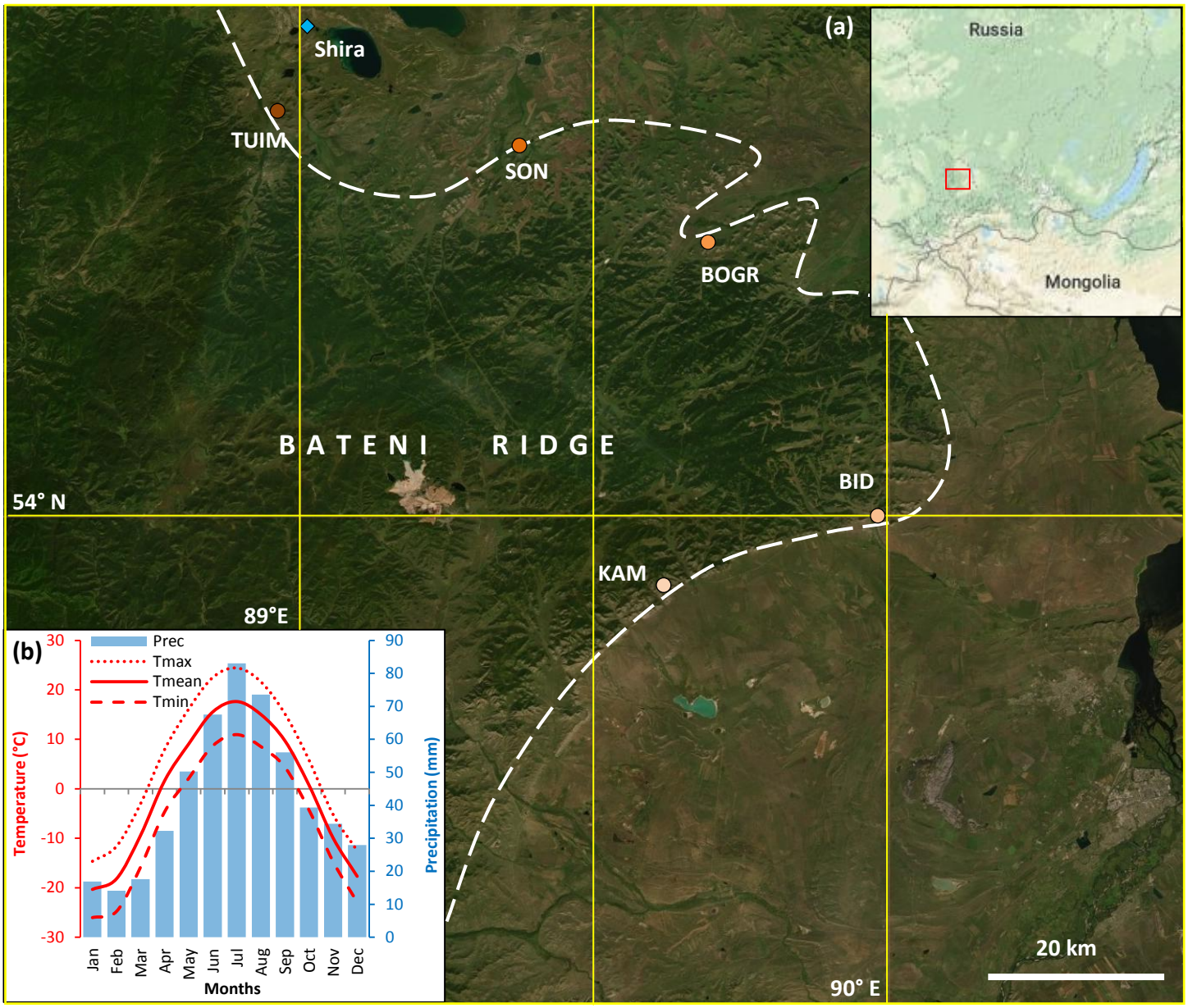

Fig. 1. Study region. (a) Satellite map of the area 53.5-54.5°N 89.5-91.5°E prepared using the ArcGIS online map tool (https://www.arcgis.com/home/webmap/viewer.html),showing the geographic grid (yellow solid lines), the approximate boundary of the Bateni Ridge (dashed line), the location of the Shira weather station (diamond) and the sampling sites (circles with a gradient of color along the transect in the foothills). (b) Monthly climatic diagram averaged from CRU TS 4.02 for the area shown on the map

To analyze the radial growth of Siberian larch, five sampling sites in 30-50 km from each other in the forest-steppe zone along the foothills of the Bateni Ridge were chosen (Fig. 1a, Table 1, Fig. S1). The selected sites were on sunlit slopes oriented southwest to southeast. Larch prevails on the western part of the ridge, presenting as standalone trees on the background of steppe vegetation at the TUIM site and dominating in the mixed larch-birch forest stands at the KAM and SON sites. At the eastern tip of the ridge at the BOGR and BID sites, there are mixed forest stands consisting of all three species.

142 **Table 1.** Characteristics of sampling sites and tree-ring width (TRW) chronologies

Characteristics	TUIM	SON	BOGR	BID	KAM	**BAT**
Sampling site						
latitude (N)	54°24'20"	54°21'55"	54°15'58"	54°00'20"	53°55'52"	–
longitude (E)	89°57'27"	90°22'04"	90°41'30"	90°58'52"	90°37'30"	–
elevation, m a.s.l.	550-600	530-600	550-620	640-670	700-770	–
Sample						
number of trees	84	55	44	68	61	**312**
length, years	301	168	175	316	310	**316**
cover period, years	1719-2019	1851-2018	1845-2019	1704-2019	1710-2019	**1704-2019**
average TRW	1.265	1.174	0.935	1.228	0.924	**1.127**
Residual TRW chronology						
standard deviation	0.399	0.383	0.314	0.283	0.357	**0.288**
mean inter-series correlation	0.496	0.569	0.500	0.469	0.451	**0.372**
mean sensitivity	0.462	0.427	0.353	0.330	0.380	**0.329**
EPS>0.85 from calendar year	1744	1889	1882	1815	1759	**1758**

143

144 *2.2 Climatic data*

145 The spatially distributed field Climate Research Unit Time-Series (CRU TS 4.02,
146 Harris et al., 2014), which includes monthly series of minimum, mean, and maximum
147 temperature (*Tmin*, *Tmean*, *Tmax*) and precipitation (*P*), and the fields of monthly drought
148 indices *SPEI* (Beguería et al., 2014) and *PDSI* (Osborn et al., 2018) were used as the main
149 sources of climatic data in this study. In 1936, the methodology used in meteorological
150 observations in Russia was changed, and the number of reference weather stations
151 increased sharply (NCDC, 2005); we thus limited analysis of climatic series to the period
152 1936-2019, the period for which the observations are of maximum reliability. The spatial
153 climatic gradients in the study area were determined from the initial field at a resolution of
154 0.5×0.5° on the geographical grid, and we used series averaged for the entire Bateni Ridge
155 territory (53.5-54.5°N 89.5-91.5°E) to perform dendroclimatic analysis and identification
156 of the regional climatic trends. During the analysis, monthly climatic series were
157 generalized (averaged or, in case of precipitation, summed) to determine the impact of
158 seasonal climatic conditions on larch growth. In addition, daily temperature and
159 precipitation data from the Shira weather station (54°30'N 89°56'E, north of the study
160 area) were used to examine the climatic regimes of certain years in detail.

161 *2.3 Dendrochronological data*

162 Wood samples (cores) of adult living larch trees were collected at breast height
163 (~1.3 m), one core per tree, and processed using standard dendrochronology techniques

(Cook and Kairiukstis, 1990). Individual series of tree-ring width (TRW) were measured at the LINTAB station using the TSAP program (Rinn, 2003) and cross-dated; the cross-dating was verified using the COFECHA program (Holmes, 1983). Then, in the ARSTAN program (Cook and Krusic, 2005), the age trends were fitted by a cubic smoothing spline with a frequency response of 0.50 at 67% of the individual series length, than the age trends and autocorrelations were removed from the raw series, making it possible to isolate high-frequency fluctuations (including the climatic signal) to obtain residual indexed series. The individual series were averaged based on bi-weighted means to obtain generalized chronologies for each site separately. The regional chronology for the entire transect along the Bateni Ridge foothills (BAT) was obtained by averaging the individual series from all sites.

2.4 Statistical analysis

The following statistics of TRW chronologies were used in the study: standard deviation (*SD*), mean sensitivity (Fritts, 1976), mean inter-serial correlation coefficient (Cook, 1985), and expressed population signal (*EPS*, Wigley et al., 1984). Despite recent discussion of the applicability of mean sensitivity in dendrochronological research from a statistical point of view (e.g., Bunn et al., 2013), this characteristic has ecological value, for example, in regard to the risk of tree mortality under conditions of severe stress (Gillner et al., 2013; Macalady and Bugmann, 2014).

To identify the relationships between TRW chronologies and climatic factors, paired correlation coefficients and a multifactor linear regression model were used. The threshold values of $mean \pm SD$ and $mean \pm 1.5SD$ (Schweingruber et al., 1990; cf. Neuwirth et al., 2007) were used to identify extremes in larch growth (pointer years) and climatic variables (droughts and the most favorable conditions).

To analyze the stability of larch growth under drought stress, the indices proposed by Lloret et al. (2011) were used: resistance ($Rt = G_d/G_{prev}$), recovery ($Rc = G_{post}/G_d$) and resilience ($Rs = G_{post}/G_{prev}$), where G_{prev} is the average growth during the 3 years prior to the drought, G_d is the average growth during the drought, and G_{post} is the average growth during the 3 years following the drought (see comparison of 2-, 3-, and 4-year periods in Gazol et al., 2017). The average values of TRW at the site calculated from the generalized raw chronologies were used as an indicator of larch growth (cf. Merlin et al., 2015; Gazol

et al., 2017), since many cores had rotted pith or pith offset, making it difficult to calculate the basal increment area as in Lloret et al. (2011).

3 Results

3.1 Radial growth chronologies of larch and their statistics

The obtained site chronologies of larch TRW have lengths of 168–316 years. Trees older than 200 years are mainly observed at the TUIM and KAM sites (Table 1, Fig. S2); the forest stands in the northeastern part of the ridge (the SON, BOGR, BID sites) are younger. The average radial growth varies moderately among the sites, amounting to 0.9–1.3 mm per year. The statistical characteristics of the residual chronologies indicate a rather high general (standard deviation 0.28–0.40) and year-to-year variability (mean sensitivity 0.33–0.46) in combination with a substantial common signal (inter-serial correlations 0.45–0.57, EPS > 0.85 for the entire period of climatic observations).

All site chronologies are closely correlated with each other (0.62–0.80, Table 2); this made it possible to build a regional chronology BAT for the Bateni Ridge foothills. The variability and the common signal characteristics of the regional chronology are lower than those of the site chronologies; however, they remain sufficient for use in dendroclimatic analysis.

Table 2. Correlations between residual TRW chronologies for 1936-2019

Site	TUIM	SON	BOGR	BID	KAM
SON	0.80				
BOGR	0.71	0.77			
BID	0.63	0.62	0.67		
KAM	0.72	0.76	0.72	0.75	
BAT	**0.80**	**0.90**	**0.86**	**0.82**	**0.89**

All correlation coefficients are significant at $p<0.00001$.

3.2 Climate-growth relationships

Correlation dendroclimatic analysis of site TRW chronologies with monthly climatic series showed that among the temperature variables during the previous and current vegetative seasons, the limitation of larch growth was most pronounced for the *Tmax* series (Table S1). A significant response to the temperature from July to September of the previous season and to the temperature in May and July of the current season was observed (Fig. 2). At the same time, precipitation, *SPEI* and other moisture-related

climatic variables from June to September of the previous season and, to a lesser extent, from April to July of the current season stimulated larch growth. A positive reaction to precipitation during the previous November was also observed.

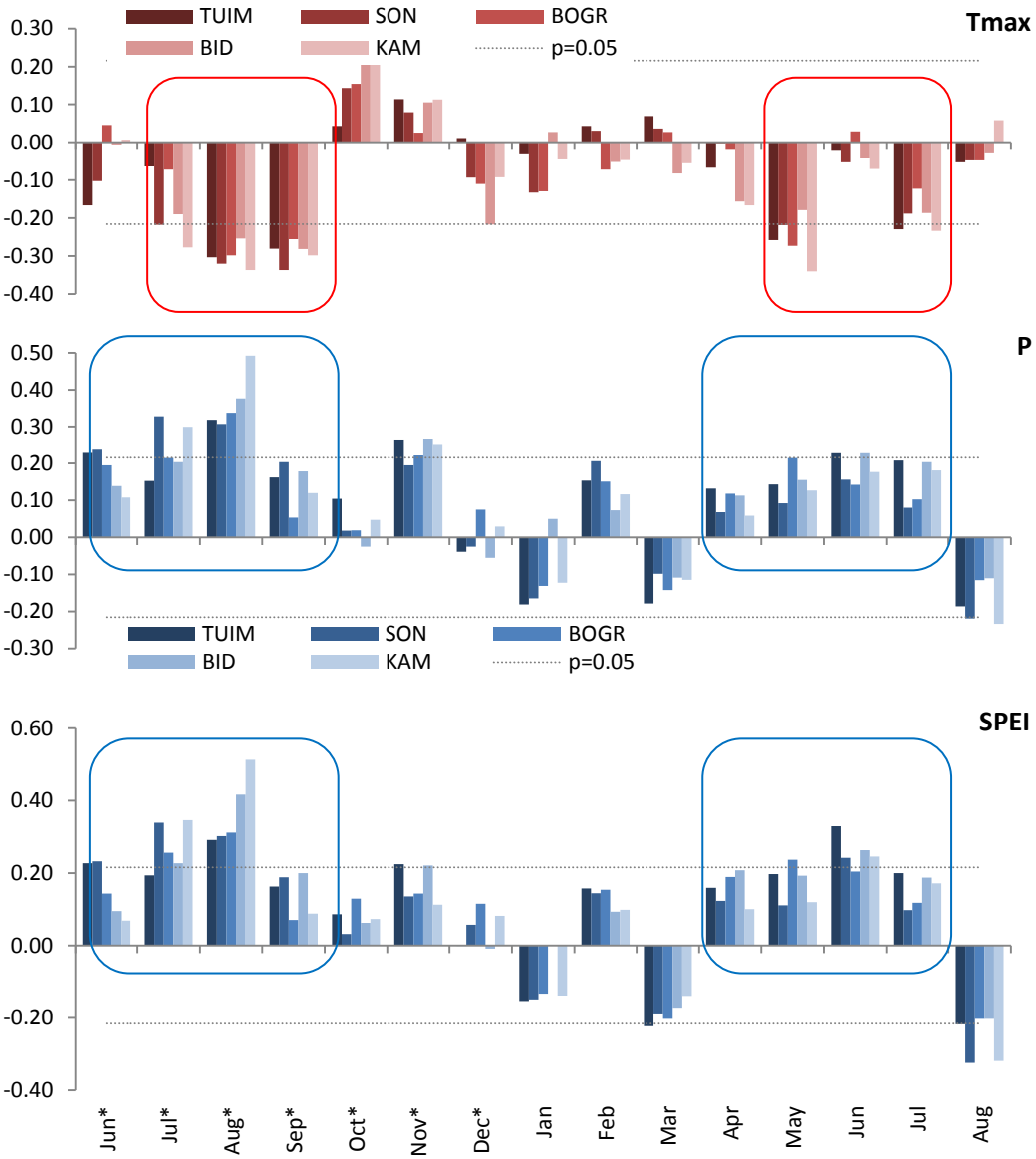

Fig 2. Correlations of site TRW chronologies with monthly maximum temperature, precipitation, and *SPEI*. On the horizontal axis, asterisks mark the months of the previous year (i.e., the year preceding tree ring formation)

After generalizing the climatic factors for the second half of the previous vegetative season and the first half of the current vegetative season, maximum correlations of the TRW chronologies with temperature were obtained for the previous July–September and the current May–July; in both cases, the most pronounced response to precipitation and *SPEI* started earlier: June–September and April–July (Table S2).

Since seasonal series of *SPEI* have significant correlations with larch growth but not with each other, they can be used as non-collinear predictors in a multifactor linear regression model of larch growth (Table 3). The obtained models are of high statistical significance; they account for 24–34% of the larch growth variability at a site scale and for 38% of the larch growth variability at the regional scale. The fitness of these models at all sites is higher than that of models that employ separate seasonal series of precipitation and maximum temperature (not presented). The regional model of climate-driven component in larch TRW variability, BAT = $f(SPEI_{prev}, SPEI_{curr})$, can be used as an indicator of climate aridity during the vegetative season in the study area (see Williams et al., 2013).

Table 3. Multifactor regressions between TRW chronologies and seasonal series of *SPEI* for the second part of the previous vegetative season (*prev*) and the first part of the current vegetative season (*curr*)

Site	Equation $f(SPEI)$	R^2	R^2_{adj}	F	p
TUIM	$0.939+0.294 \cdot SPEI_{prev}+0.295 \cdot SPEI_{curr}$	0.333	0.315	18.4	<0.00001
SON	$0.947+0.397 \cdot SPEI_{prev}+0.181 \cdot SPEI_{curr}$	0.324	0.306	17.7	<0.00001
BOGR	$0.953+0.262 \cdot SPEI_{prev}+0.236 \cdot SPEI_{curr}$	0.258	0.237	12.8	0.00002
BID	$0.956+0.230 \cdot SPEI_{prev}+0.214 \cdot SPEI_{curr}$	0.357	0.340	20.5	<0.00001
KAM	$0.950+0.308 \cdot SPEI_{prev}+0.166 \cdot SPEI_{curr}$	0.317	0.298	17.2	<0.00001
BAT	$\mathbf{0.949+0.298 \cdot SPEI_{prev}+0.218 \cdot SPEI_{curr}}$	**0.400**	**0.384**	**24.7**	**<0.00001**

3.3 Spatiotemporal patterns of vegetative season climatic variability

For the seasonal climatic series that were found to most significantly affect larch growth, a spatial distribution field was obtained from the corresponding monthly data for the geographical grid at a resolution of 0.5° over the study area (Fig. 3a). The spatial climatic patterns in the first and second halves of the vegetative season are similar. An increase in temperature and a decrease in precipitation, i.e., an increase in climate aridity, were observed from the TUIM to the BID sites, whereas opposite pattern was observed from the BID to the KAM sites. Because *SPEI* does not allow comparison of sites, the climate aridity at each site was estimated as the average value of *P*/*Tmax* for the *prev* and *curr* seasons:

$$\text{mean}(P / Tmax) = \text{mean}(P_{\text{Jun*-Sep*}} / Tmax_{\text{Jul*-Sep*}}; P_{\text{Apr-Jul}} / Tmax_{\text{May-Jul}}).$$

In this equation, *P* / *Tmax* were calculated from their average values for 1937-2018 interpolated by geographical coordinates. Obtained mean(*P* / *Tmax*) values are following: 13.39 mm/°C in TUIM, 12.88 mm/°C in SON, 12.53 mm/°C in BOGR, 11.44 mm/°C in BID, and 12.36 mm/°C in KAM. However, the variability of the microclimate depending

on the local landscape and the elevation at the sampling sites should also be taken into account. Note that this spatial gradient is followed by a higher variability of larch radial growth (Table 1), both in general (SD of residual chronologies) and in regard to its year-to-year component (mean sensitivity). During the cover period of reliable climatic data, precipitation during the vegetative season in the study area was stable; no significant long-term trends were observed (Fig. 3b). At the same time, the increase in the maximum temperature during the vegetative season was approximately 0.14-0.20°C per decade. As a result, the overall climate aridity also increased.

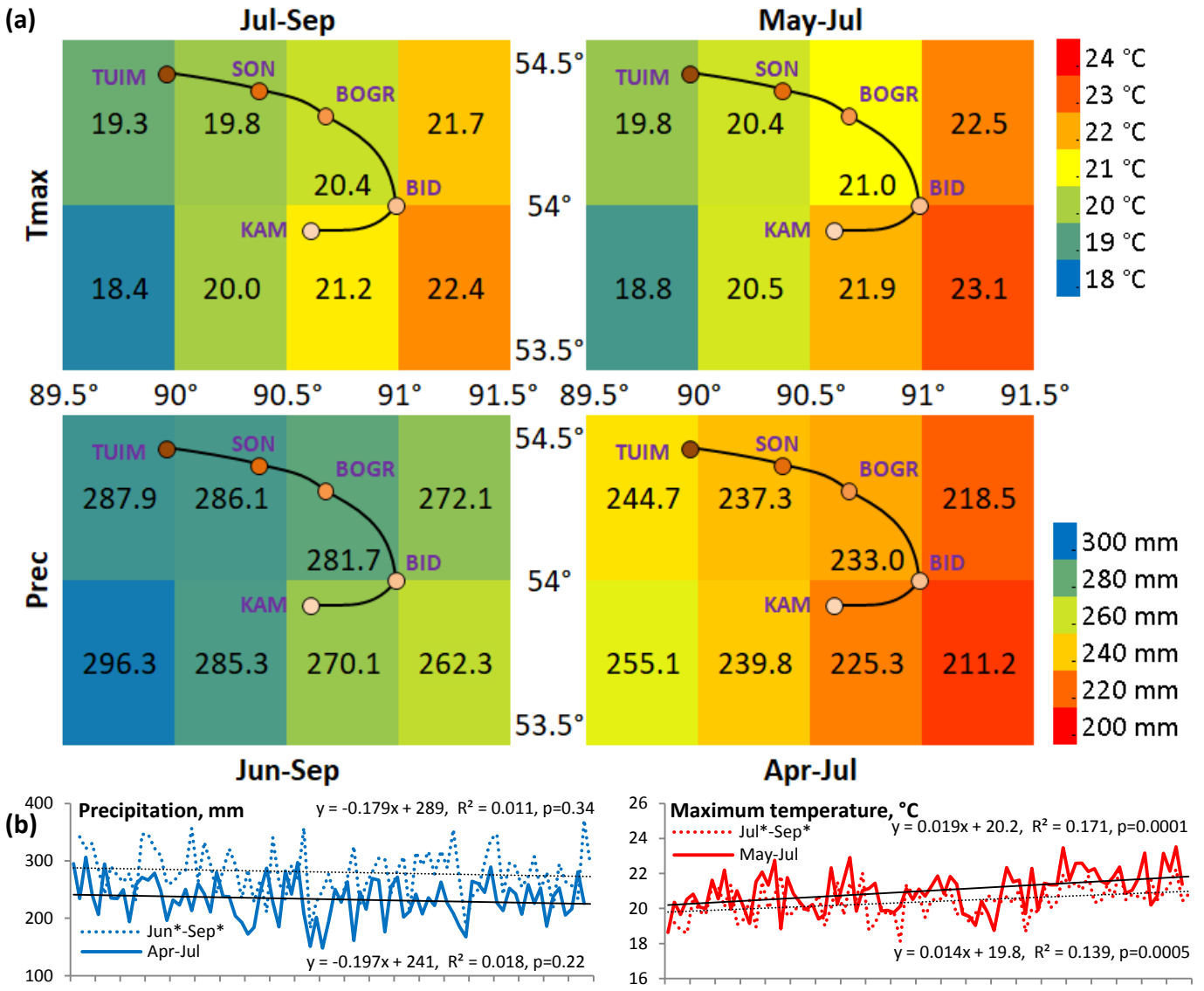

Fig. 3. Spatiotemporal patterns of the regional seasonal series of maximum temperature and precipitation, generalized over intervals of their maximal impact on tree growth (Table S2). (a) Spatial gradients of average values over the period 1936-2019 for the cells of a 0.5°×0.5° geographic grid. The connected dots represent a transect of the sampling sites along the Bateni Ridge foothills. (b) Interannual dynamics during the period 1936-2019

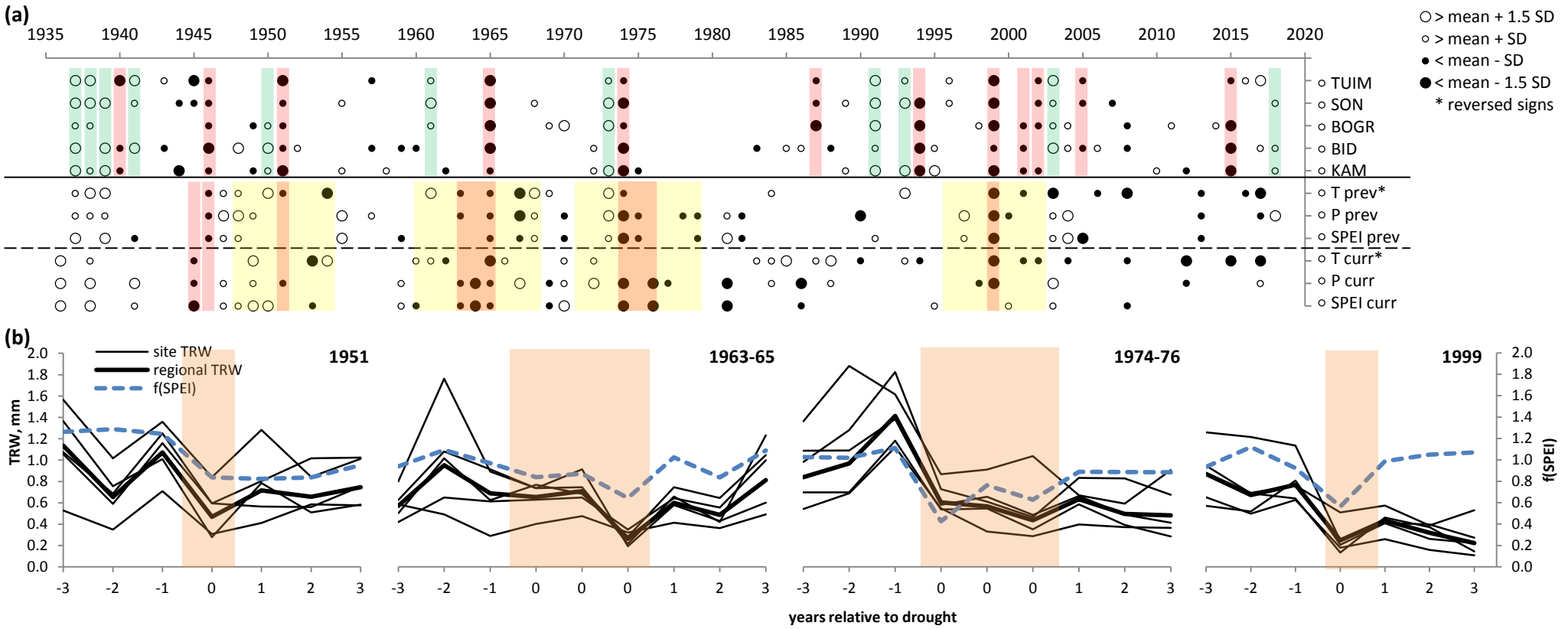

283

284

285 **Fig. 4.** Dynamics of larch growth and droughts in the study area. (a) Pointer years and climatic extremes for the period 1936-2019, differentiated by weak
286 (small markers; deviation from the mean value is 1–1.5 standard deviations) and strong (large markers; deviation from the mean value is >1.5 standard
287 deviations), positive (empty markers) and negative (filled markers). Note that the sign is reversed for maximum temperatures to take into account their negative
288 impact on tree growth, i.e., hot weather is considered a negative extreme, and cool weather is considered a positive extreme. The time intervals of the seasonal
289 climatic series (*prev* and *curr*) are the same as those in Table S2. The shaded areas in the top part of the plot represent pointer years of the regional scale, i.e.,
290 observed at >50% of the sites. The shaded areas in the bottom part of the plot represent years of droughts considered in this study and the three-year periods
291 prior to and following the droughts. (b) Larch radial growth duringdroughts and during the 3 years prior to, and following the droughts. The shaded areas
292 represent drought years. The thin and thick solid lines represent the bi-weighted mean of TRW (i.e., raw chronologies) for the sampling sites and for the region,
293 respectively. The dashed lines represent the *f*(*SPEI*) regression model (Table 3, last line) used as a regional drought index individualized for larch

294 *3.4 Dynamics of extreme events: pointer years in larch growth and droughts*

295 During the period under consideration, 11 positive and 12 negative pointer years
296 (defined as the years of the formation of extremely wide and extremely narrow rings,
297 respectively) were observed for larch growth on a regional scale, i.e., covering more than
298 half of the sampling sites along the transect (Fig. 4a). As can be seen, most of these pointer
299 years (with the exception of 1940, 1987, 1991, 1994, and 2005) coincide with extreme
300 deviations in the corresponding direction in seasonal series of precipitation, maximum
301 temperatures and/or *SPEI*. The climatic differences between positive and negative pointer
302 years are also more substantial for months during *prev* and *curr* seasons than for other
303 months (Fig. S3).

304 Data on other stress factors are available for pointer years 1990, 1994, and 2000-
305 2005 (Fig. 4). According to the daily temperature and precipitation data recorded at the
306 Shira weather station, extreme frosts (-20–25°C) were observed in November 1993 before
307 the formation of snow cover; in contrast, a warm autumn and a mild snowy winter were
308 recorded in 1990. A significant difference in the amount of precipitation during November
309 was also observed when positive and negative pointer years were compared (Fig. S3). In
310 addition, according to the State Forest Committee, in 2000-2005 large areas were affected
311 by an outbreak of gypsy moth (*Lymantria dispar* L.) on the Bateni Ridge (Fig. S4).
312 Unfortunately, no observations on the insect population dynamics in earlier years are
313 available.

314 *3.5 Stability of larch growth*

315 Among the climatic extremes that significantly suppressed larch growth on the
316 regional scale, several droughts (1951, 1963-65, 1974-76 and 1999, Fig. 4a) that occurred
317 at intervals of more than 6 years were selected. Six-year interval was chosen to avoid
318 overlapping of the three-year periods before and after drought. Despite the fact that during
319 each of the periods 1963–65 and 1974–76 only one pointer year was observed, in both
320 cases, both the radial growth of larch and *SPEI* remained substantially lower than the
321 mean values during all three years (Fig. 4b); therefore, these periods were considered as
322 three-year droughts. A comparison of larch growth dynamics and *SPEI* after droughts
323 shows that recovery of growth after a drought event occurs in accordance with climatic
324 dynamics in the cases of relatively weak drought. However, an increase in the duration of
325 adverse conditions (1963–65 and 1974–76) is accompanied by a slight divergence between

the *f*(*P/Tmax*) series and larch growth after the first year of drought. During the three years following the severe drought that occurred in 1999, growth did not recover despite relatively favorable conditions.

For each drought, three indicators characterizing the growth stability under stress, resistance *Rt*, recovery *Rc*, and resilience *Rs*, were calculated. Comparison between sites shows that *Rt* increases significantly with local climatic aridity; also, there are tendencies for *Rs* to increase and for *Rc* to decrease, both close to the significance threshold (Fig. 5a). The dependence of growth stability on the severity of drought stress is more pronounced: both *Rt* and *Rs* are closely correlated with *f*(*SPEI*) calculated on the local scale (Fig. 5b). Comparison of growth stability with climatic conditions during the 3-year periods before (for all three indices) and after drought (for *Rc* and *Rs*) did not reveal any significant relationships (p=0.22-0.85). Determination of the relationship of the stability indices to tree age, preliminarily estimated as mean cambial age for all individual series at the sites during each drought (Table S3), revealed correlations close to zero for *Rt* and *Rc*, but there was a decrease in *Rs* with age close to the significance threshold (r=0.34, p=0.14).

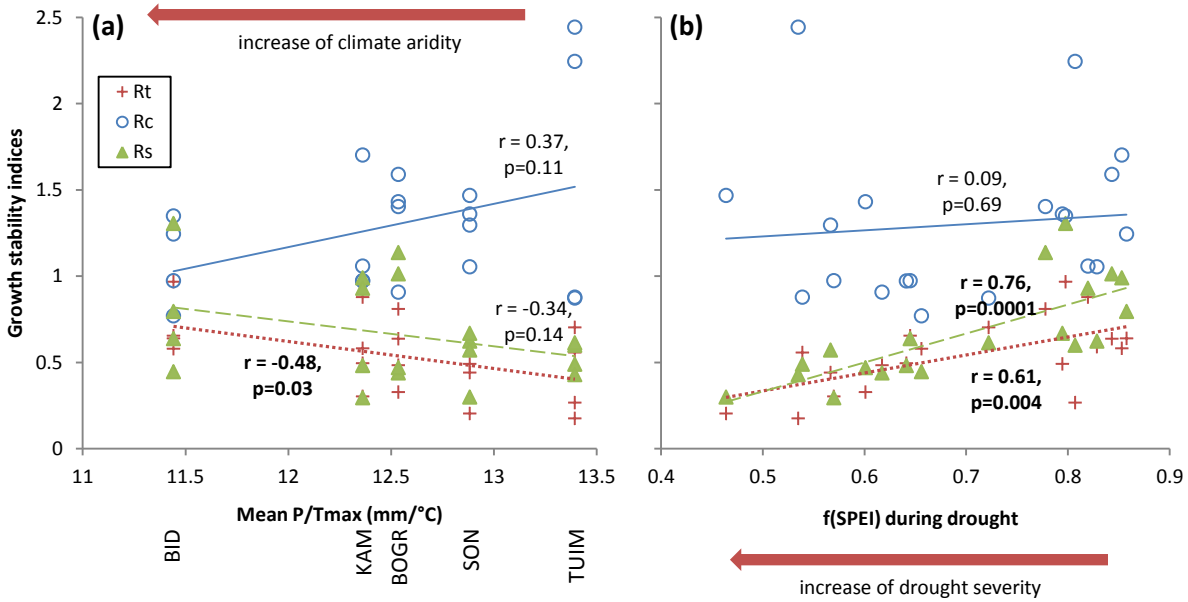

Fig. 5. Patterns in growth stability indices: *Rt*: resistance (pluses, dotted lines); *Rc*: recovery (circles, solid lines; *Rs*: resilience (triangles, dashed lines). Coefficients of determination written in bold indicate statistical significance (p<0.05) of linear relationships. (a) Relationship between growth stability indices and climate aridity at sampling sites estimated as mean *P*/*Tmax* ratio. The sites are labeled below the horizontal axis. (b) Relationships between growth stability indices and drought severity estimated at the local scale as values of regression functions *TRW*=*f*(*SPEI*) (Table 3) during the drought year or averaged for 3 years of drought.

4 Discussion

Despite the substantial territory of the study area (the maximum distance between the sampling sites is more than 150 km), the presence of common signals in the dynamics of larch growth allow us to consider the entire forest-steppe ecotone of the Bateni Ridge as a single geographical object characterized by a unity of fluctuations in environmental conditions and a common response of vegetation to these fluctuations. At the same time, tree-ring width chronologies are a promising indicator of the long-term dynamics of this ecosystem state, and this dynamics is relevant to regional forest management in the context of the ongoing climate change.

Siberian larch, on one hand, is sufficiently drought-tolerant to permit it to grow on the lower forest boundary in the study area; on the other hand, it is highly sensitive to climatic conditions in terms of climate-driven growth variation (sf. Dulamsuren et al., 2009). The plasticity of larch growth is ensured by the species' ecophysiological features. Its shorter duration of xylogenesis compared to that of evergreen conifers (Gower and Richards, 1990; Rossi et al., 2006; Velisevich and Khutornoy, 2009; Kraus et al., 2016) and its high intensity of metabolism, even under conditions of moisture deficit, due to its anisohydric strategy (McDowell et al. 2008; Martínez-Vilalta et al., 2014), lead to the maintenance of a high rate of photosynthesis during short-term droughts. During longer period of water stress, partial abscission of needles and fine roots (Chenlemuge et al., 2015; Khansaritoreh et al., 2018) protects the body of the tree from damage without lasting effects on growth, unlike evergreen species. In addition, larch has a relatively narrow sapwood (1–2 cm or 10–15 rings, Bergstedt and Lyck, 2007), a trait that accelerates the acclimation of the stem hydraulic architecture to long-term climatic trends.

The negative reaction of radial growth to temperature and the positive reaction to precipitation during the warm season, revealed by correlation dendroclimatic analysis and comparison of climatic conditions during the pointer years, is typical for trees growing in moisture-limited regions (Stahle et al., 2011; Touchan et al., 2011; Wu et al., 2013; Cook et al., 2016; Kurz-Besson et al., 2016; Shestakova et al., 2016 and others), but climatic response obviously has species- and region-specific seasonality and intensity. The more pronounced and stable response of chronologies to the maximum temperature during the vegetative season can be explained by the fact that the water stress that suppresses tree growth reaches its maximal levels in the daytime, when higher air temperatures (including

the daily maximum) are combined with solar radiation, and additional substantial heating of the soil and foliage occurs (Jackson et al., 1981; Wieser, 2007; Ermida et al., 2014). A similar dependence of tree growth on maximal temperature and precipitation in other regions has been described quantitatively (e.g., Williams et al., 2013). The predominance of the response to conditions of the previous vegetative season is probably due to the large input of accumulated non-structural assimilates in the growth of larch, a deciduous species with an intensive growth strategy (Kozlowski 1992; Hoch et al., 2003; Pallardy 2007; Piper, Fajardo, 2014). Despite the low winter precipitation, the positive effect of November precipitation on growth can be substantial, probably due to thermal insulation by the snow cover formed during that months; this is supported by climatic observations for the pointer years 1990 and 1993.

There are no obvious spatial gradients in the climatic response of larch. This can be explained by the complex interaction between the gradients of climatic variables, local landscape conditions (e.g., microclimate modifiers), forest stand density, differences between pure and mixed stands, etc. (Martínez-Vilalta et al., 2012; Lebourgeois et al., 2012 2013; Pretzsch et al., 2015; Thurm et al., 2016). Nevertheless, moisture availability should be relatively similar at all sampling sites because all sites are located near the forest-steppe boundary, the position of which (e.g., elevation at slopes of different orientation) is mostly defined by moisture limitation of tree growth. Unfortunately, the limited cover period of direct observations on forest disturbances and their drivers does not allow us to determine the causes of growth depression during some pointer years. However, the identified depression of larch growth during the massive gypsy moth outbreak in 2000-2005 is a striking example of the fact that, in addition to direct exposure, drought can have a long-term indirect effect through the demographic regulation of insects and the increased vulnerability of trees (McDowell et al., 2008 and references therein). However, our observation that larch growth was relatively rapid in wetter and cooler years during this outbreak (Fig. S4) supports the high resilience of deciduous larch to defoliation (Hoch et al., 2003; Piper, Fajardo, 2014; Foster, 2017). It should also be taken into account that larch has a competitive advantage in mixed stands containing evergreen pine for several years after defoliation, since the gypsy moth feeds on both species.

The correspondence between the spatial gradients in climate aridity and the resistance/resilience of larch growth can be associated with genetic adaptation and with

morphological acclimation of trees to permanent moisture deficit through formation of appropriate hydraulic architecture and alterations in the proportion of foliage, fine roots and sapwood areas, changes that reduce the trees' sensitivity to increased water stress (Martínez-Vilalta et al. 2008, 2012; Anderegg et al. 2013, 2015). This assumption is supported by the corresponding gradients in the standard deviation and especially in mean sensitivity of the TRW chronologies, since these characteristics are associated with greater risk of mortality under drought stress (Gillner et al., 2013; Macalady and Bugmann, 2014). Resilience decreases more rapidly and has a stronger relationship to severity of drought than resistance; thus severe droughts have more long-term effects on larch growth.

Despite the fact that radial growth decreases with age (Table S3, also compare plots from left to right in Fig. 4b), in this study it was found that the sensitivity of larch to droughts depends primarily on drought intensity, although the possibility of increasing tree vulnerability to drought with age and size should also be taken into account (cf. Lloret et al., 2011; Serra-Maluquer et al., 2018). This was reflected on the local scale as a nearly significant decrease in resilience. However, local chronologies are averaged from the radial growth series of trees of various ages, that are growing under various micro-conditions of habitat, occupy different social position in the forest stand, and have different growth rates, genotypes and other individual characteristics; therefore, the analysis of generalized chronologies does not allow us to judge the contribution of these factors with any accuracy. Growth stability under the influence of drought can depend significantly on all these factors (Velisevich and Khutornoy, 2009; Kuznetsova and Kozlov, 2011; Bennett et al., 2015; Merlin et al., 2015; Serra‐Maluquer et al., 2018); for example, drought resistance may increase and recovery may decrease with soil moisture and slope (Gazol et al., 2017). In this regard, it would be interesting to continue the study of larch growth stability in more detail, taking into account the scale of individual trees. A large sample size (number of trees, Table 1) at several sampling sites will make it possible to use mixed linear models to identify the contributions of factors on the individual to regional scales to larch growth stability in the study area. Investigation of the responses of individual trees to periodic stresses caused by droughts and/or biotic agents is of particular interest for understanding forest acclimation and adaptation to a changing environment. The results of such a study can be used for forest management in the study area and in

particular for planning measures for forest conservation and/or reforestation considering further regional climate warming.

Acknowledgments

The study was supported by the Russian Science Foundation (project no. 19-14-00120, additional sampling and dendrochronological analysis; project no. 19-77-30015, spatial analysis).

References

Alisov, B.P., 1956. Climate of the USSR. Moscow State University, Moscow (In Russian).

Allen, C.D., Macalady, A.K., Chenchouni, H., Bachelet, D., McDowell, N., Vennetier, M., Kitzberger, T., Rigling, A., Breshears, D.D., Hogg, E.H., Gonzalez, P., Fensham, R., Zhang, Z., Castro, J., Demidova, N., Lim, J.H., Allard, G., Running, S.W., Semerci, A., Cobb, N., 2010. A global overview of drought and heat-induced tree mortality reveals emerging climate change risks for forests. For. Ecol. Manag. 259 (4), 660–684. https://doi.org/10.1016/j.foreco.2009.09.001.

Allen, C.D., Breshears, D.D., McDowell, N.G., 2015. On underestimation of global vulnerability to tree mortality and forest die-off from hotter drought in the Anthropocene. Ecosphere 6 (8), 129. https://doi.org/10.1890/es15-00203.1.

Anderegg, W.R.L., Plavcová, L., Anderegg, L.D.L., Hacke, U., Berry, J.A., Field, C.B., 2013. Drought's legacy: multiyear hydraulic deterioration underlies widespread aspen forest die-off and portends increased future risk. Glob. Change Biol. 19 (4), 1188–1196. https://doi.org/10.1111/gcb.12100.

Anderegg, W.R.L., Schwalm, C., Biondi, F., Camarero, J.J., Koch, G., Litvak, M., Ogle, K., Shaw, J.D., Shevliakova, E., Williams, A.P., Wolf, A., Ziaco, E., Pacala, S., 2015. Pervasive drought legacies in forest ecosystems and their implications for carbon cycle models. Science 349 (6247), 528–532. https://doi.org/10.1126/science.aab1833.

Anderegg, L.D.L., HilleRisLambers, J., 2016. Drought stress limits the geographic ranges of two tree species via different physiological mechanisms. Glob. Change Biol. 22 (3), 1029–1045. https://doi.org/10.1111/gcb.13148.

Barber, V.A., Juday, G.P., Finney, B.P., 2000. Reduced growth of Alaskan white spruce in the twentieth century from temperature-induced drought stress. Nature 405 (6787), 668–673. https://doi.org/10.1038/35015049.

Bazhenova, O.I., Tyumentseva, E.M., 2010. The structure of contemporary denudation in the steppes of the Minusinskaya depression. Geogr. Nat. Resour. 31 (4), 362–369. htpps://doi.org/10.1016/j.gnr.2010.11.010.

Beguería, S., Vicente-Serrano, S.M., Reig, F., Latorre, B., 2014. Standardized Precipitation Evapotranspiration Index (SPEI) revisited: parameter fitting, evapotranspiration models, kernel weighting, tools, datasets and drought monitoring. Int. J. Clim. 34, 3001–3023. htpps://doi.org/10.1002/joc.3887.

Bennett, A.C., McDowell, N.G., Allen, C.D., Anderson-Teixeira, K.J., 2015. Larger trees suffer most during drought in forests worldwide. Nature Plants 1, 15139. https://doi.org/10.1038/nplants.2015.139.

Bergstedt, A., Lyck, C. (Eds.), (2007). Larch Wood – a Literature Review. Forest & Landscape Denmark, Copenhagen.

Bigler, C., Bräker, O.U., Bugmann, H., Dobbertin, M., Rigling, A., 2006. Drought as an inciting mortality factor in Scots pine stands of the Valais, Switzerland. Ecosyst. 9 (3), 330–343. https://doi.org/10.1007/s10021-005-0126-2.

Bocharov, A.Y., Savchuk, D.A. (2015). Structure of forests and climatic response of trees in "forest-steppe" contact zone, the Altai Mountains. J. Sib. Fed. Univ. Biol. 8 (4), 426–440. https://doi.org/10.17516/1997-1389-2015-8-4-426-440. (In Russian).

Bunn, A.G., Jansma, E., Korpela, M., Westfall, R D., Baldwin, J., 2013. Using simulations and data to evaluate mean sensitivity (ζ) as a useful statistic in dendrochronology. Dendrochronologia 31(3), 250-254. https://doi.org/10.1016/j.dendro.2013.01.004.

Cailleret, M., Jansen, S., Robert, E.M.R., Desoto, L., Aakala, T., Antos, J.A., Beikircher, B., Bigler, C., Bugmann, H., Caccianiga, M., Cada, V., Camarero, J.J., Cherubini, P., Cochard, H., Coyea, M.R., Cufar, K., Das, A.J., Davi, H., Delzon, S., Dorman, M., Gea-Izquierdo, G., Gillner, S., Haavik, L.J., Hartmann, H., Heres, A.M., Hultine, K.R., Janda, P., Kane, J.M., Kharuk, V.I., Kitzberger, T., Klein, T., Kramer, K., Lens, F., Levanic, T., Linares Calderon, J.C., Lloret, F., Lobo-Do-Vale, R., Lombardi, F., López Rodriguez, R., Mäkinen, H., Mayr, S., Mészáros, I., Metsaranta, J.M., Minunno, F.,

509 Oberhuber, W., Papadopoulus, A., Peltoniemi, M., Petritan, A.M., Rohner, B., Sangüesa-
510 Barreda, G., Sarris, D., Smith, J.M., Stan, A.B., Sterck, F., Stojanovic, D.B., Suarez, M.L.,
511 Svoboda, M., Tognetti, R., Torres-Ruiz, J.M., Trotsiuk, V., Villalba, R., Vodde, F.,
512 Westwood, A.R., Wyckoff, P.H., Zafirov, N., Martínez-Vilalta, J., 2017. A synthesis of
513 radial growth patterns preceding tree mortality. Glob. Change Biol. 23 (4), 1675–1690.
514 https://doi.org/10.1111/gcb.13535.

515 Camarero, J.J., Manzanedo, R.D., Sanchez-Salguero, R., Navarro-Cerrillo, R.M.,
516 2013. Growth response to climate and drought change along an aridity gradient in the
517 southernmost *Pinus nigra* relict forests. Ann. For. Sci. 70 (8), 769–780.
518 https://doi.org/10.1007/s13595-013-0321-9.

519 Chen, P.Y., Welsh, C., Hamann, A., 2010. Geographic variation in growth response
520 of Douglas-fir to interannual climate variability and projected climate change. Glob.
521 Change Biol. 16 (12), 3374–3385. https://doi.org/10.1111/j.1365-2486.2010.02166.x.

522 Chenlemuge, T., Schuldt, B., Dulamsuren, C., Hertel, D., Leuschner, C., Hauck, M.,
523 2015. Stem increment and hydraulic architecture of a boreal conifer (*Larix sibirica*) under
524 contrasting macroclimates. Trees 29 (3), 623–636. https://doi.org/10.1007/s00468-014-
525 1131-x.

526 Clark, J.S., Iverson, L., Woodall, C.W., Allen, C.D., Bell, D.M., Bragg, D.C.,
527 D'Amato, A.W., Davis, F.W., Hersh, M.H., Ibanez, I., Jackson, S.T., Matthews, S.,
528 Pederson, N. Peters, M., Schwartz, M.W., Waring, K.M., Zimmermann, N.E., 2016. The
529 impacts of increasing drought on forest dynamics, structure, and biodiversity in the United
530 States. Glob. Change Biol. 22 (7), 2329–2352. https://doi.org/10.1111/gcb.13160.

531 Cook, E.R., 1985. A Time Series Analysis Approach to Tree-Ring Standardization.
532 PhD thesis. Univ. of Arizona, Tucson.

533 Cook, E.R., Kairiukstis, L.A., 1990. Methods of Dendrochronology: Applications in
534 the Environmental Sciences. Springer, Dordrecht. htpps://doi.org/10.1007/978-94-015-
535 7879-0.

536 Cook, E.R., Krusic, P.J., 2005. Program ARSTAN: a Tree-Ring Standardization
537 Program Based on Detrending and Autoregressive Time Series Modeling, with Interactive
538 Graphics. Lamont-Doherty Earth Observatory, Columbia University, Palisades.

Cook, B.I., Anchukaitis, K.J., Touchan, R., Meko, D.M., Cook, E.R., 2016. Spatiotemporal drought variability in the Mediterranean over the last 900 years. J. Geophys. Res. Atmos. 121 (5), 2060–2074. https://doi.org/10.1002/2015JD023929.

Dai, A., Trenberth, K.E., Karl, T.R., 1998. Global variations in droughts and wet spells: 1900–1995. Geophys. Res. Lett. 25 (17), 3367–3370. https://doi.org/10.1029/98GL52511.

Dai, A., 2013. Increasing drought under global warming in observations and models. Nature Clim. Change 3, 52–58. https://doi.org/10.1038/nclimate1633.

Delucia, E.H., Maherali, H., Carey, E.V., 2000. Climate-driven changes in biomass allocation in pines. Glob. Change Biol. 6, 587–593. https://doi.org/10.1046/j.1365-2486.2000.00338.x.

Dorman, M., Svoray, T., Perevolotsky, A., Sarris, D., 2013. Forest performance during two consecutive drought periods: diverging long-term trends and short-term responses along a climatic gradient. For. Ecol. Manag. 310, 1–9. https://doi.org/10.1016/j.foreco.2013.08.009.

Dorman, M., Perevolotsky, A., Sarris, D., Sarris, D., 2015. The effect of rainfall and competition intensity on forest response to drought: lessons learned from a dry extreme. Oecol. 177 (4), 1025–1038. https://doi.org/10.1007/s00442-015-3229-2.

Dulamsuren C., Hauck M., Bader M., Osokhjargal D., Oyungerel S., Nyambayar S., Runge M., Leuschner C., 2009. Water relations and photosynthetic performance in *Larix sibirica* growing in the forest-steppe ecotone of northern Mongolia. Tree Physiol. 29 (1), 99–110. https://doi.org/10.1093/treephys/tpn008.

Dulamsuren, C., Khishigjargal, M., Leuschner, C., Hauck, M., 2013. Response of tree-ring width to climate warming and selective logging in larch forests of the Mongolian Altai. J. Plant Ecol. 7 (1), 24–38. https://doi.org/10.1093/jpe/rtt019.

Engelbrecht, B.M.J., Comita, L.S., Condit, R., Kursar, T.A., Tyree, M.T., Turner, B.L., Hubbell, S.P., 2007. Drought sensitivity shapes species distribution patterns in tropical forests. Nature 447, 80–82. https://doi.org/10.1038/nature05747.

Ermida, S.L., Trigo, I.F., DaCamara, C.C., Göttsche, F.M., Olesen, F.S., Hulley, G., 2014. Validation of remotely sensed surface temperature over an oak woodland landscape – The problem of viewing and illumination geometries. Remote Sens. Environ. 148, 16–27. https://doi.org/10.1016/j.rse.2014.03.016.

Fritts, H.C., 1976. Tree Rings and Climate. Academic Press, London.

Foster, J.R., 2017. Xylem traits, leaf longevity and growth phenology predict growth and mortality response to defoliation in northern temperate forests. Tree Physiol. 37 (9), 1151–1165. https://doi.org/10.1093/treephys/tpx043.

Galiano, L., Martínez-Vilalta, J., Lloret, F., 2011. Carbon reserves and canopy defoliation determine the recovery of Scots pine 4 yr after a drought episode. New Phytol. 190 (3), 750–759. https://doi.org/10.1111/j.1469-8137.2010.03628.x.

Gazol, A., Camarero, J.J., Anderegg, W.R.L., Vicente-Serrano, S.M., 2017. Impacts of droughts on the growth resilience of Northern Hemisphere forests. Glob. Ecol. Biogeogr. 26 (2), 166–176. https://doi.org/10.1111/geb.12526.

Gillner, S., Rüger, N., Roloff, A., Berger, U., 2013. Low relative growth rates predict future mortality of common beech (*Fagus sylvatica* L.). For. Ecol. Manag. 302, 372-378. https://doi.org/10.1016/j.foreco.2013.03.032.

Gower, S.T., Richards, J.H., 1990. Larches: deciduous conifers in an evergreen world. BioSci. 40 (11), 818–826. https://doi.org/10.2307/1311484.

Harris, I., Jones, P.D., Osborn, T.J., Lister, D.H., 2014. Updated high-resolution grids of monthly climatic observations – the CRU TS3.10 Dataset. Int. J. Climatol. 34 (3), 623–642. htpps://doi.org/10.1002/joc.3711.

Hoch, G., Richter, A., Körner, C., 2003. Non-structural carbon compounds in temperate forest trees. Plant Cell Environ. 26 (7), 1067–1081. https://doi.org/10.1046/j.0016-8025.2003.01032.x.

Holmes, R.L., 1983. Computer-assisted quality control in tree-ring dating and measurement. Tree-Ring Bull. 43, 69–78.

Jackson, R.D., Idso, S.B., Reginato, R.J., Pinter Jr., P.J., 1981. Canopy temperature as a crop water stress indicator. Water Resour. Res. 17 (4), 1133–1138. https://doi.org/10.1029/WR017i004p01133.

Khansaritoreh, E., Schuldt, B., Dulamsuren, C., 2018. Hydraulic traits and tree-ring width in *Larix sibirica* Ledeb. as affected by summer drought and forest fragmentation in the Mongolian forest steppe. Ann. For. Sci. 75, 30. https://doi.org/10.1007/s13595-018-0701-2.

Kozlowski, T.T., 1992. Carbohydrate sources and sinks in woody plants. Bot. Rev. 58 (2), 107–222. https://doi.org/10.1007/BF02858600.

Kraus, C., Zang, C., Menzel, A., 2016. Elevational response in leaf and xylem phenology reveals different prolongation of growing period of common beech and Norway spruce under warming conditions in the Bavarian Alps. Eur. J. For. Res. 135 (6), 1011–1023. https://doi.org/10.1007/s10342-016-0990-7.

Kulagin, A.Y., Davydychev, A.N., Zaitsev, G.A. (2006) Specific features of the growth of Siberian spruce (*Picea obovata* Ledeb.) at early stages of ontogeny in broadleaf-conifer forests of the Ufa plateau. Russ. J. Ecol. 37 (1), 66–69. https://doi.org/10.1134/S1067413606010115.

Kurz-Besson, C.B., Lousada, J.L., Gaspar, M.J., Correia, I.E., David, T.S., Soares, P.M.M., Cardoso, R.M., Russo, A., Varino, F., Mériaux, C., Trigo, R.M., Gouveia, C.M., 2016. Effects of recent minimum temperature and water deficit increases on *Pinus pinaster* radial growth and wood density in southern Portugal. Front. Plant Sci. 7, 1170. https://doi.org/10.3389/fpls.2016.01170.

Kuznetsova, E.P., Kozlov, D.N., 2011. Tree-ring variability of larch (Larix Sibirica Ledeb.) in different landscape positions of the Terekhol depression, Tuva, Russia in the 20th Century. J. Sib. Fed. Univ. Biol. 4 (4), 325–337 (In Russian).

Lange, J., Cruz-García, R., Gurskaya, M., Jalkanen, R., Seo, J.-W., & Wilmking, M., 2016. Can microsite effects explain divergent growth in treeline Scots pine? In: Hevia, A., Sánchez-Salguero, R., Linares, J.C., Olano, J.M., Camarero, J.J., Gutiérrez, E., Helle, G., Gärtner, H. (Eds.), Proceedings of the DENDROSYMPOSIUM 2015: May 20th - 23rd, 2015 in Sevilla, Spain, (Scientific Technical Report; 16/04), 14th TRACE conference (Tree Rings in Archaeology, Climatology and Ecology) (Sevilla, Spain 2015). GFZ German Research Centre for Geosciences, Potsdam, pp. 93–101. http://doi.org/10.2312/GFZ.b103-16042.

Lebourgeois, F., Gomez, N., Pinto, P., Mérian, P., 2013. Mixed stands reduce *Abies alba* tree-ring sensitivity to summer drought in the Vosges mountains, western Europe. For. Ecol. Manag. 303, 61–71. https://doi.org/10.1016/j.foreco.2013.04.003.

Lei, Y., Liu, Y., Song, H., Sun, B., 2014. A wetness index derived from tree-rings in the Mt. Yishan area of China since 1755 AD and its agricultural implications. Chin. Sci. Bull. 59 (27), 3449–3456. https://doi.org/10.1007/s11434-014-0410-7.

Levesque, M., Rigling, A., Bugmann, H., Weber, P., Brang, P., 2014. Growth response of five co-occurring conifers to drought across a wide climatic gradient in

635 Central Europe. Agric. For. Meteorol. 197, 1–12.
636 https://doi.org/10.1016/j.agrformet.2014.06.001.
637 Lloret, F., Keeling, E. G., Sala, A., 2011. Components of tree resilience: effects of
638 successive low-growth episodes in old ponderosa pine forests. Oikos 120 (12), 1909–1920.
639 https://doi.org/10.1111/j.1600-0706.2011.19372.x.
640 Lyu, S., Wang, X., Zhang, Y., Li, Z., 2017. Different responses of Korean pine
641 (*Pinus koraiensis*) and Mongolia oak (*Quercus mongolica*) growth to recent climate
642 warming in northeast China. Dendrochronologia 45, 113–122.
643 https://doi.org/10.1016/j.dendro.2017.08.002.
644 Macalady, A.K., Bugmann, H., 2014. Growth-mortality relationships in piñon pine
645 (*Pinus edulis*) during severe droughts of the past century: shifting processes in space and
646 time. PLoS One 9(5), e92770. https://doi.org/10.1371/journal.pone.0092770.
647 Maherali, H., Pockman, W.T., Jackson, R.B., 2004. Adaptive variation in the
648 vulnerability of woody plants to xylem cavitation. Ecol. 85 (8), 2184–2199.
649 https://doi.org/10.1890/02-0538.
650 Martínez-Vilalta, J., Lopez, B.C., Adell, N., Badiella, L., Ninyerola, M., 2008.
651 Twentieth century increase of Scots pine radial growth in NE Spain shows strong climate
652 interactions. Glob. Change Biol. 14, 2868–2881. https://doi.org/10.1111/j.1365-
653 2486.2008.01685.x.
654 Martinez-Vilalta, J., Cochard, H., Mencuccini, M., Streck, F., Herrero, A.,
655 Korhonen, J.F.J., Llorens, P., Nikinmaa, E., Nolè, A., Poyatos, R., Ripullone, F., Sass-
656 Klaassen, U., Zweifel R., 2009. Hydraulic adjustment of Scots pine across Europe. New
657 Phytol. 184 (2), 353–364. https://doi.org/10.1111/j.1469-8137.2009.02954.x.
658 Martínez-Vilalta, J., López, B.C., Loepfe, L., Lloret, F., 2012. Stand- and tree-level
659 determinants of the drought response of Scots pine radial growth. Oecol. 168 (3), 877–
660 888. https://doi.org/10.1007/s00442-011-2132-8.
661 Martínez-Vilalta, J., Poyatos, R., Aguadé, D., Retana, J., Mencuccini, M., 2014. A
662 new look at water transport regulation in plants. New Phytol. 204 (1), 105–115.
663 https://doi.org/10.1111/nph.12912.
664 McDowell, N., Pockman, W.T., Allen, C.D., Breshears, D.D., Cobb, N., Kolb, T.,
665 Plaut, J., Sperry, J., West, A., Williams, D.G., Yepez, E.A., 2008. Mechanisms of plant
666 survival and mortality during drought: why do some plants survive while others succumb

667 to drought? New Phytol. 178 (4), 719–739. https://doi.org/10.1111/j.1469-
668 8137.2008.02436.x.
669 McDowell, N.G., Allen, C.D., Marshall, L., 2010. Growth, carbon-isotope
670 discrimination, and drought-associated mortality across a *Pinus ponderosa* elevational
671 transect. Glob. Change Biol. 16 (1), 399–415. https://doi.org/10.1111/j.1365-
672 2486.2009.01994.x.
673 Merlin, M., Perot, T., Perret, S., Korboulewsky, N., Vallet, P., 2015. Effects of stand
674 composition and tree size on resistance and resilience to drought in sessile oak and Scots
675 pine. For. Ecol. Manag. 339, 22–33. https://doi.org/10.1016/j.foreco.2014.11.032.
676 Monnier, Y., Prévosto, B., Ripert, C., Corbani, A.C., Fernandez, C., 2012. Forest
677 microhabitats differentially influence seedling phenology of two co-existing
678 Mediterranean oak species. J. Veg. Sci. 23 (2), 260–270. https://doi.org/10.1111/j.1654-
679 1103.2011.01358.x.
680 National Climatic Data Center (NCDC), 2005. Data Documentation for Dataset
681 9290c, Global Synoptic Climatology Network. C. The former USSR, Version 1.0.
682 National Climatic Data Center, Asheville. (Available at
683 https://www1.ncdc.noaa.gov/pub/data/documentlibrary/tddoc/td9290c.pdf; accessed 04
684 October 2019).
685 Neuwirth, B., Schweingruber, F.H., Winiger, M., 2007. Spatial patterns of central
686 European pointer years from 1901 to 1971. Dendrochronologia 24 (2–3), 79–89.
687 https://doi.org/10.1016/j.dendro.2006.05.004.
688 Osborn, T.J., Barichivich, J., Harris, I., van der Schrier, G., Jones, P.D., 2018.
689 Drought [in "State of the Climate in 2017"]. Bull. Am. Meteorol. Soc. 99, S36–S37.
690 https://doi.org/10.1175/2018BAMSStateoftheClimate.1.
691 Pallardy, S.G., 2007. Physiology of Woody Plants. Academic Press, San Diego,.
692 Pasho, E., Camarero, J.J., de Luis, M., Vicente-Serrano, S.M., 2011. Impacts of
693 drought at different time scales on forest growth across a wide climatic gradient in north-
694 eastern Spain. Agric. For. Meteorol. 151 (12), 1800–1811.
695 https://doi.org/10.1016/j.agrformet.2011.07.018.
696 Peñuelas, J., Filella, I., Lloret, F., Piñol, J. Siscart, D., 2000. Effects of a severe
697 drought on water and nitrogen use by *Quercus ilex* and *Phyllyrea latifolia*. Biol. Plant. 43
698 (1), 47–53. https://doi.org/10.1023/A:1026546828466.

Piper, F.I., Fajardo, A., 2014. Foliar habit, tolerance to defoliation and their link to carbon and nitrogen storage. J. Ecol. 102 (5), 1101–1111. https://doi.org/10.1111/1365-2745.12284.

Pretzsch, H., del Río, M., Ammer, Ch., Avdagic, A., Barbeito, I., Bielak, K., Brazaitis, G., Coll, L., Dirnberger, G., Drössler, L., Fabrika, M., Forrester, D.I., Godvod, K., Heym, M., Hurt, V., Kurylyak, V., Löf, M., Lombardi, F., Matović, B., Mohren, F., Motta, R., den Ouden, J., Pach, M., Ponette, Q., Schütze, G., Schweig, J., Skrzyszewski, J., Sramek, V., Sterba, H., Stojanović, D., Svoboda, M., Vanhellemont, M., Verheyen, K., Wellhausen, K., Zlatanov, T., Bravo-Oviedo, A., 2015. Growth and yield of mixed versus pure stands of Scots pine (*Pinus sylvestris* L.) and European beech (*Fagus sylvatica* L.) analysed along a productivity gradient through Europe. Eur. J. For. Res. 134 (5), 927–947. https://doi.org/10.1007/s10342-015-0900-4.

Rinn, F., 2003. TSAP-Win: Time Series Analysis and Presentation for Dendrochronology and Related Applications: User reference. RINNTECH, Heidelberg.

Rossi, S., Rathgeber, C.B.K., Deslauriers, A., 2009. Comparing needle and shoot phenology with xylem development on three conifer species in Italy. Ann. For. Sci. 66 (2), 206. https://doi.org/10.1051/forest/2008088.

Schweingruber, F.H., Eckstein, D., Serre-Bachet, F., Braker, O.U., 1990. Identification, presentation and interpretation of event years and pointer years in dendrochronology. Dendrochronologia 8, 9–38.

Shestakova, T.A., Gutiérrez E., Kirdyanov, A.V., Camarero, J.J., Génova, M., Knorre, A.A., Linares, J.C., de Dios, V.R., Sánchez-Salguero, R., Voltas, J., 2016. Forests synchronize their growth in contrasting Eurasian regions in response to climate warming. Proc. Natl. Acad. Sci. 113 (3), 662–667. https://doi.org/10.1073/pnas.1514717113.

Seager, R., Ting, M., Held, I., Kushnir, Y., Lu, J., Vecchi, G., Huang, H.-P., Harnik, N., Leetmaa, A., Lau, N.-C., Li, C., Velez, J., Naik, N., 2007. Model projections of an imminent transition to a more arid climate in southwestern North America. Sci. 316 (5828), 1181–1184. https://doi.org/10.1126/science.1139601.

Selyaninov, G.T., 1928. About climate agricultural estimation. Proc. Agric. Meteorol. 20, 165–177 (In Russian).

Serra-Maluquer, X., Mencuccini, M., Martínez-Vilalta, J., 2018. Changes in tree resistance, recovery and resilience across three successive extreme droughts in the

731 northeast Iberian Peninsula. Oecol. 187 (1), 343–354. https://doi.org/10.1007/s00442-018-
732 4118-2.
733 Stahle, D.W., Diaz, J.V., Burnette, D.J., Paredes, J.C., Heim Jr., R.R., Fye, F.K.,
734 Acuna Soto, R., Therrell, M.D., Cleaveland, M.K., Stahle, D.K., 2011. Major
735 Mesoamerican droughts of the past millennium. Geophys. Res. Lett. 38 (5), L05703.
736 https://doi.org/10.1029/2010GL046472.
737 Touchan, R., Woodhouse, C.A., Meko, D.M., Allen, C., 2011. Millennial
738 precipitation reconstruction for the Jemez Mountains, New Mexico, reveals changing
739 drought signal. Int. J. Climatol. 31 (6), 896–906. https://doi.org/10.1002/joc.2117.
740 Thurm, E.A., Uhl, E., Pretzsch, H., 2016. Mixture reduces climate sensitivity of
741 Douglas-fir stem growth. For. Ecol. Manag. 376, 205–220.
742 https://doi.org/10.1016/j.foreco.2016.06.020.
743 Velisevich, S.N., Khutornoy, O.V., 2009. Effects of climatic factors on radial
744 growth of Siberian stone pine and Siberian larch in sites with different soil humidity in the
745 south of Western Siberia. J. Sib. Fed. Univ. Biol. 2(1), 117–132 (In Russian).
746 Wieser, G., 2007. Climate at the upper timberline. In: Wieser, G., Tausz, M. (Eds.).
747 Trees at Their Upper Limit: Treelife Limitation at the Alpine Timberline. Springer,
748 Dordrecht. pp. 19–36.
749 Wilhite, D.A., 1993. Drought Assessment, Management and Planning: Theory and
750 Case Studies. Kluwer, Boston, MA.
751 Williams, A.P., Allen, C.D., Macalady, A.K., Griffin D., Woodhouse, C.A.,
752 Meko, D.M., Swetnam, T.W., Rauscher, S.A., Seager, R., Grissino-Mayer, H.D., Dean,
753 J.S., Cook, E.R., Gangodagamage, C., Cai, M., McDowell, N.G., 2013. Temperature as a
754 potent driver of regional forest drought stress and tree mortality. Nat. Clim. Change 3,
755 292–297. https://doi.org/10.1038/nclimate1693.
756 Wigley, T.M.L., Briffa, K.R., Jones, P.D., 1984. On the average value of correlated
757 time series, with applications in dendroclimatology and hydrometeorology. J. Appl.
758 Meteorol. Climatol. 23 (2), 201–213. https://doi.org/10.1175/1520-
759 0450(1984)023<0201:OTAVOC>2.0.CO;2.
760 World Meteorological Organization (WMO) and Global Water Partnership (GWP),
761 2016: Handbook of Drought Indicators and Indices (Eds. M. Svoboda and B.A. Fuchs).

762 Integrated Drought Management Programme (IDMP), Integrated Drought Management
763 Tools and Guidelines Series 2. Geneva.
764 Wu, X., Liu, H., Wang, Y., Deng, M., 2013. Prolonged limitation of tree growth due
765 to warmer spring in semi-arid mountain forests of Tianshan, northwest China. Environ.
766 Res. Lett. 8 (2), 024016. htpps://doi.org/10.1088/1748-9326/8/2/024016.
767 Yatagai, A, Yasunari, T., 1995. Interannual variations of summer precipitation in the
768 arid/semi-arid regions in China and Mongolia: Their regionality and relation to the Asian
769 summer monsoon. J. Meteorol. Soc. Jpn. Ser. II, 73 (5), 909–923.
770 htpps://doi.org/10.2151/jmsj1965.73.5_909.
771

To which side are the scales swinging? Growth stability of Siberian larch under permanent moisture deficit with periodic droughts

Dina F. Zhirnova, Elena A. Babushkina, Liliana V. Belokopytova, Eugene A. Vaganov

Supplementary Materials

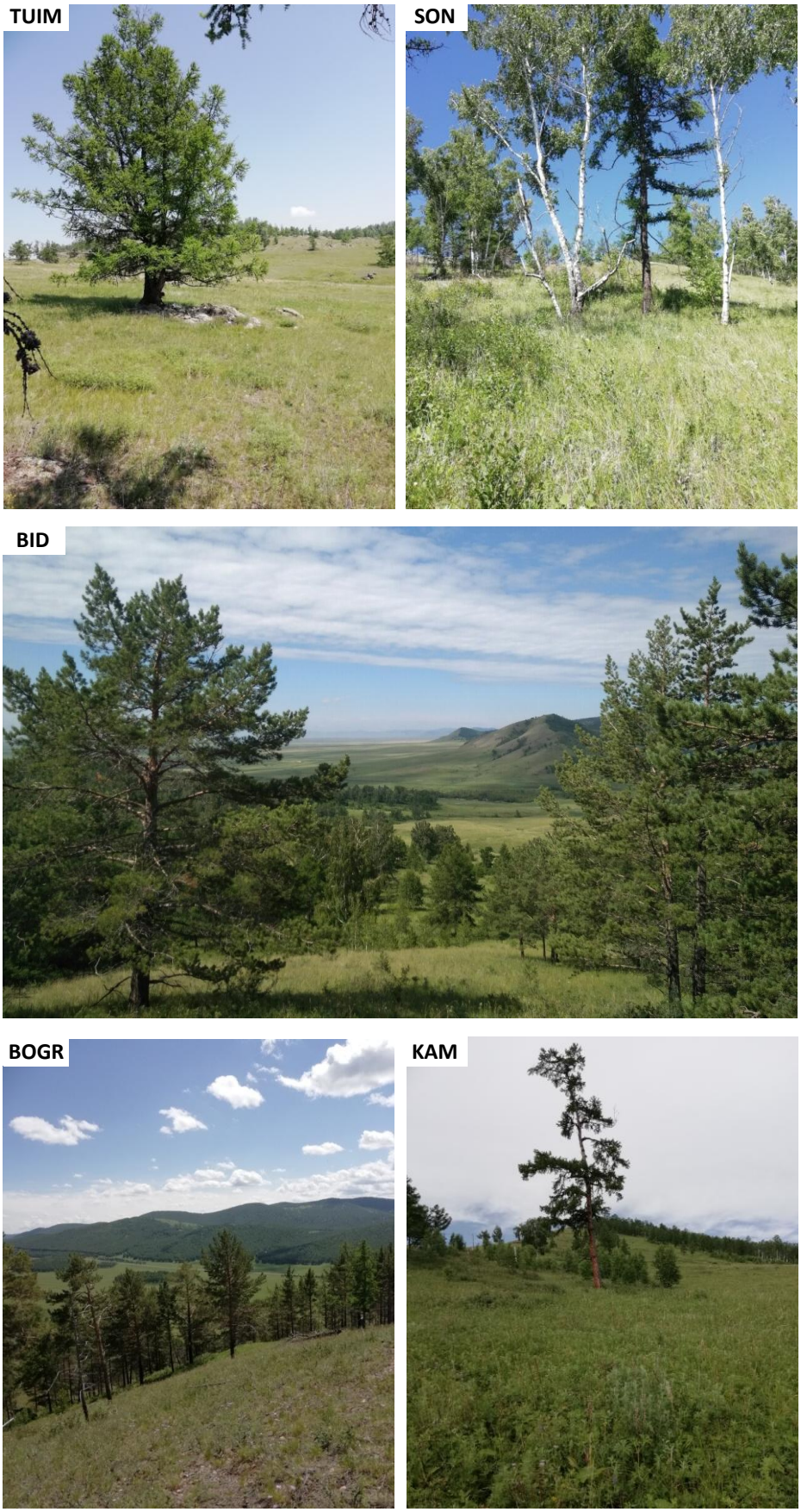

Fig. S1. Sampling sites

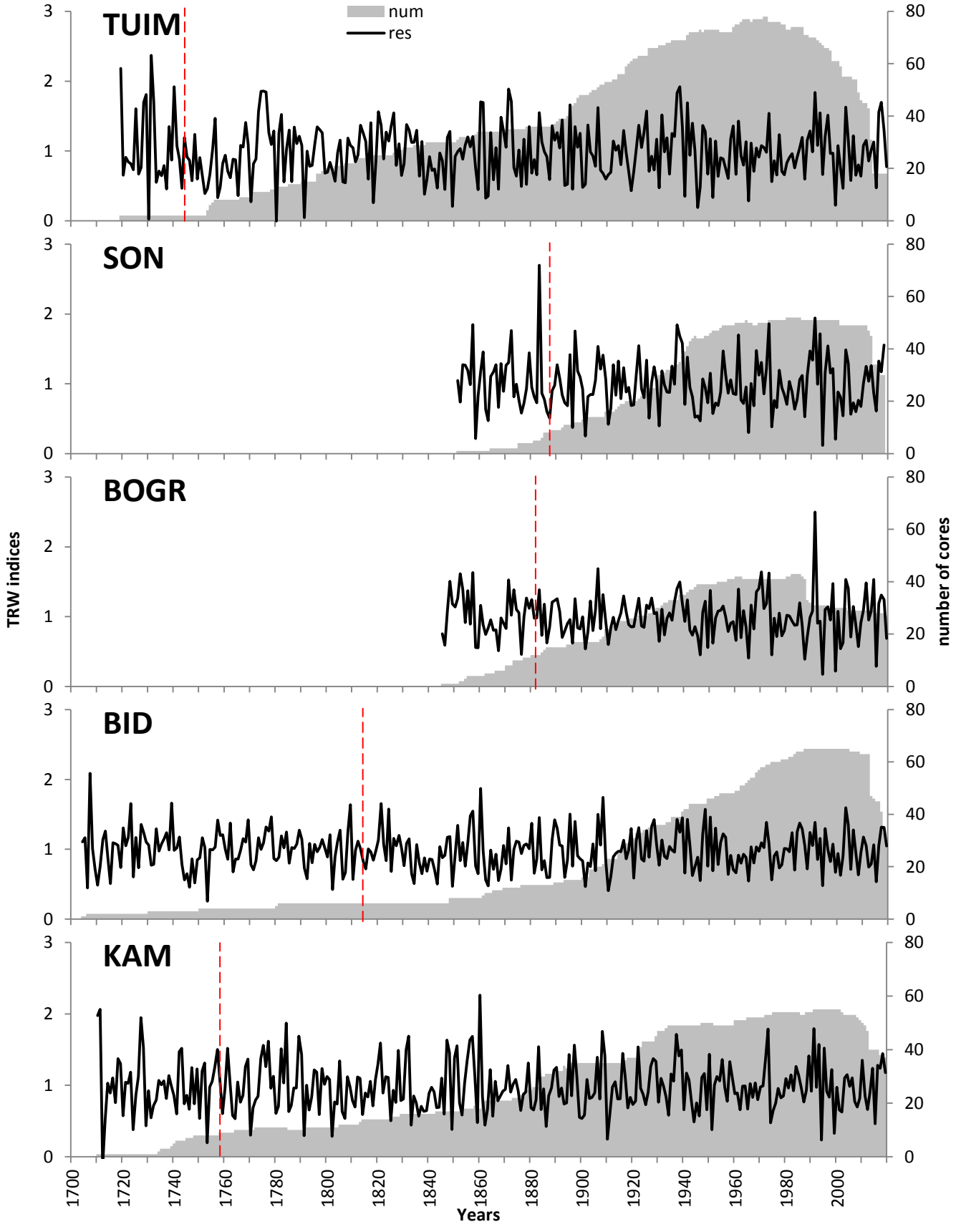

Fig. S2. Site residual TRW chronologies (lines) and respective sample depths (shades). The vertical dashed lines mark the beginning of the period with EPS>0.85. The recent decrease in sample size was caused by repeated sampling (first sampling in 2012-2013 or 1989 and second sampling in 2017-2019) to extend the cover period

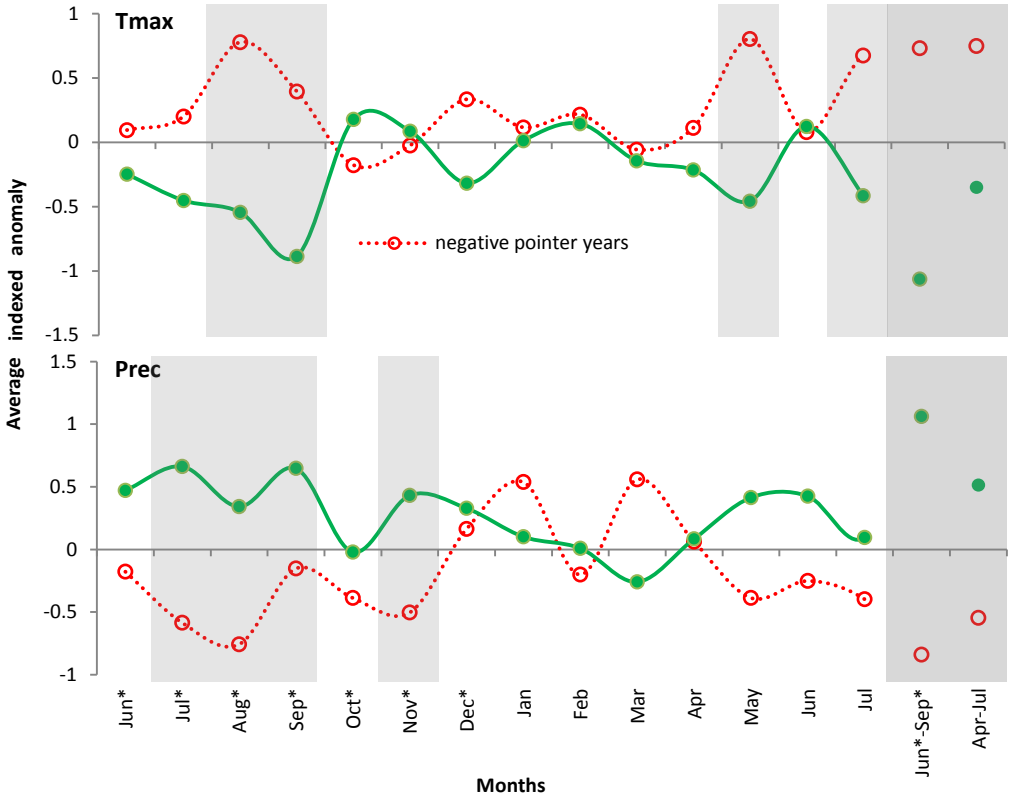

Fig. S3. Climatic patterns for pointer years of the regional scale (marked in Fig. 4). The indexed anomalies of climatic variables (maximum temperature or precipitation) was calculated by subtraction of the series mean value, division by the standard deviation, and then averaging separately values for positive and negative pointer years. Shaded areas mark months and seasons when differences between groups of positive and negative pointer years are significant at $p<0.05$

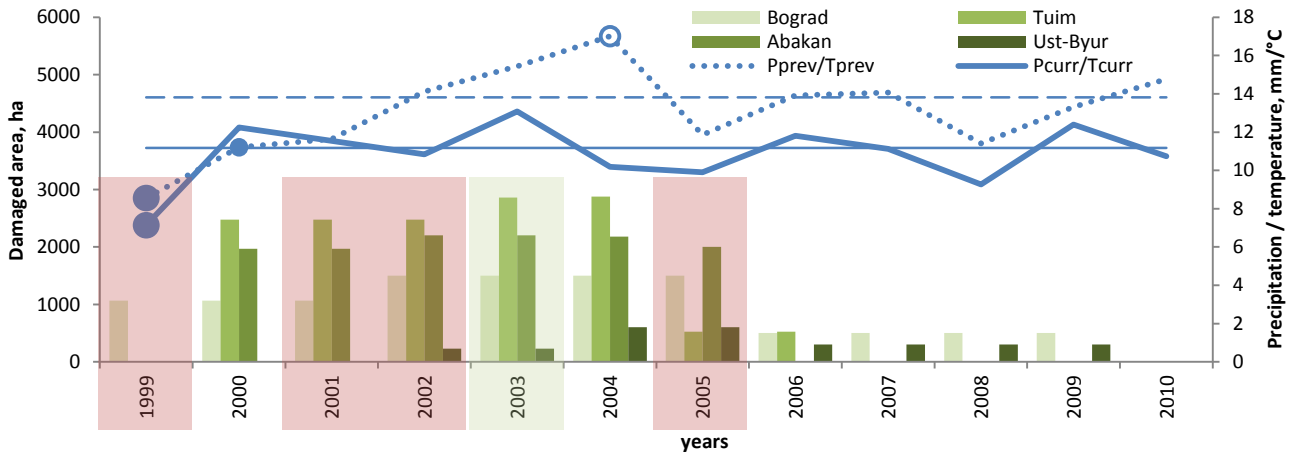

Fig. S4. Area damaged by gypsy moth (*Lymantria dispar* L.) after the severe drought of 1999 in forestries located on the territory of the Bateni Ridge. Bars represent damaged area in each forestry; lines represent seasonal series of precipitation to maximum temperature ratio P_{prev}/T_{prev} (dashed) and P_{curr}/T_{solid} (dashed) with marked extremes (see Fig. 4a); thin horizontal lines represent their respective mean values; shades represent positive (lighter green) and negative (darker red) pointer years in larch growth. Note that during period of gypsy moth outbreak, the years when larch growth is relatively rapid are associated with high P/T ratio values during the current vegetative season (2000), the previous vegetative season (2004), or both (2003).

Table S1. Correlations of site TRW chronologies with monthly climatic variables

Chronology	Month														
	Jun*	Jul*	Aug*	Sep*	Oct*	Nov*	Dec*	Jan	Feb	Mar	Apr	May	Jun	Jul	Aug
Tmin															
TUIM	-0.19	0.03	-0.14	-0.19	0.09	0.12	-0.01	-0.05	0.10	0.07	-0.02	-0.21	0.03	-0.10	-0.10
SON	-0.14	-0.08	-0.15	-0.21	0.14	0.05	-0.13	-0.14	0.09	0.04	0.02	-0.17	0.01	-0.12	-0.16
BOGR	-0.02	0.03	-0.17	-0.20	0.17	0.00	-0.14	-0.16	-0.02	0.02	0.02	**-0.23**	0.06	-0.05	-0.15
BID	-0.07	-0.10	-0.08	-0.12	0.19	0.10	**-0.22**	-0.03	-0.01	-0.08	-0.13	-0.09	0.04	-0.10	-0.17
KAM	-0.06	-0.14	-0.10	-0.16	**0.25**	0.11	-0.10	-0.07	0.01	-0.03	-0.17	**-0.24**	0.00	-0.14	-0.10
BAT	-0.12	-0.07	-0.15	-0.20	0.18	0.10	-0.12	-0.09	0.05	0.02	-0.07	-0.21	0.02	-0.13	-0.16
Tmean															
TUIM	-0.18	-0.03	**-0.26**	**-0.27**	0.07	0.12	0.00	-0.04	0.07	0.07	-0.05	**-0.25**	0.00	-0.18	-0.08
SON	-0.12	-0.17	**-0.27**	**-0.32**	0.15	0.06	-0.11	-0.13	0.06	0.04	0.01	-0.20	-0.03	-0.16	-0.10
BOGR	0.02	-0.03	**-0.26**	**-0.26**	0.17	0.01	-0.13	-0.14	-0.05	0.02	0.00	**-0.26**	0.04	-0.09	-0.09
BID	-0.03	-0.16	-0.20	**-0.24**	0.21	0.10	**-0.22**	0.00	-0.03	-0.08	-0.15	-0.15	-0.01	-0.16	-0.09
KAM	-0.02	**-0.23**	**-0.26**	**-0.28**	**0.24**	0.11	-0.10	-0.06	-0.02	-0.04	-0.17	**-0.31**	-0.04	-0.20	0.00
BAT	-0.09	-0.15	**-0.28**	**-0.32**	0.18	0.10	-0.11	-0.08	0.02	0.01	-0.09	**-0.27**	-0.02	-0.20	-0.09
Tmax															
TUIM	-0.17	-0.06	**-0.30**	**-0.28**	0.04	0.11	0.01	-0.03	0.04	0.07	-0.07	**-0.26**	-0.02	**-0.23**	-0.05
SON	-0.10	**-0.22**	**-0.32**	**-0.34**	0.14	0.08	-0.09	-0.13	0.03	0.04	0.00	**-0.22**	-0.05	-0.19	-0.05
BOGR	0.05	-0.07	**-0.30**	**-0.26**	0.15	0.03	-0.11	-0.13	-0.07	0.03	-0.02	**-0.27**	0.03	-0.12	-0.05
BID	-0.01	-0.19	**-0.25**	**-0.28**	0.21	0.11	**-0.22**	0.03	-0.05	-0.08	-0.16	-0.18	-0.04	-0.19	-0.03
KAM	0.01	**-0.28**	**-0.34**	**-0.30**	0.21	0.11	-0.09	-0.05	-0.05	-0.05	-0.17	**-0.34**	-0.07	**-0.23**	0.06
BAT	-0.07	-0.19	**-0.34**	**-0.34**	0.16	0.11	-0.10	-0.07	-0.01	0.01	-0.10	**-0.29**	-0.05	**-0.23**	-0.03
Precipitation															
TUIM	**0.23**	0.15	**0.32**	0.16	0.10	**0.26**	-0.04	-0.18	0.15	-0.18	0.13	0.14	**0.23**	0.21	-0.19
SON	**0.24**	**0.33**	**0.31**	0.20	0.02	0.19	-0.03	-0.16	0.21	-0.10	0.07	0.09	0.16	0.08	**-0.22**
BOGR	0.20	0.22	**0.34**	0.05	0.02	**0.22**	0.07	-0.13	0.15	-0.14	0.12	0.21	0.14	0.10	-0.12
BID	0.14	0.20	**0.38**	0.18	-0.03	**0.27**	-0.06	0.05	0.07	-0.11	0.11	0.16	**0.23**	0.20	-0.11
KAM	0.11	**0.30**	**0.49**	0.12	0.05	**0.25**	0.03	-0.12	0.12	-0.12	0.06	0.13	0.18	0.18	**-0.23**
BAT	0.21	**0.27**	**0.41**	0.17	0.05	**0.27**	-0.01	-0.13	0.16	-0.14	0.11	0.17	**0.22**	0.19	-0.21
SPEI															
TUIM	**0.23**	0.19	**0.29**	0.16	0.09	**0.22**	0.00	-0.15	0.16	-0.22	0.16	0.20	**0.33**	0.20	-0.22
SON	**0.23**	**0.34**	**0.30**	0.19	0.03	0.14	0.06	-0.15	0.14	-0.19	0.12	0.11	**0.24**	0.10	**-0.32**
BOGR	0.14	**0.26**	**0.31**	0.07	0.13	0.14	0.12	-0.13	0.15	-0.20	0.19	**0.24**	0.20	0.12	-0.20
BID	0.10	**0.23**	**0.42**	0.20	0.06	0.22	-0.01	0.00	0.09	-0.17	0.21	0.19	**0.26**	0.19	-0.20
KAM	0.07	**0.35**	**0.51**	0.09	0.07	0.11	0.08	-0.14	0.10	-0.14	0.10	0.12	**0.25**	0.17	**-0.32**
BAT	0.18	**0.30**	**0.41**	0.16	0.09	0.20	0.05	-0.13	0.15	-0.21	0.18	0.19	**0.31**	0.18	**-0.29**
PDSI															
TUIM	0.10	0.15	**0.30**	**0.34**	**0.36**	**0.40**	**0.39**	**0.35**	**0.37**	**0.33**	**0.39**	**0.43**	**0.47**	**0.48**	**0.36**
SON	0.11	**0.25**	**0.38**	**0.41**	**0.41**	**0.43**	**0.43**	**0.38**	**0.38**	**0.34**	**0.36**	**0.38**	**0.40**	**0.37**	0.21
BOGR	0.00	0.11	**0.25**	**0.27**	**0.27**	**0.30**	**0.31**	**0.29**	**0.30**	**0.26**	**0.30**	**0.38**	**0.39**	**0.39**	**0.28**
BID	0.14	0.24	**0.40**	**0.45**	**0.46**	**0.49**	**0.48**	**0.47**	**0.45**	**0.41**	**0.45**	**0.48**	**0.52**	**0.56**	**0.42**
KAM	0.07	0.22	**0.43**	**0.44**	**0.44**	**0.46**	**0.46**	**0.42**	**0.42**	**0.38**	**0.40**	**0.44**	**0.45**	**0.44**	0.27
BAT	0.09	0.21	**0.39**	**0.43**	**0.44**	**0.47**	**0.47**	**0.43**	**0.44**	**0.40**	**0.44**	**0.49**	**0.52**	**0.52**	**0.36**
Hydrothermal coefficient of Selyaninov (*HTC*)															
TUIM	**0.30**	0.20	**0.23**	**0.24**								0.18	0.13	0.17	-0.16
SON	**0.26**	**0.31**	**0.23**	**0.28**								0.14	0.07	0.04	-0.14
BOGR	0.15	**0.22**	**0.32**	0.11								**0.29**	0.01	0.07	-0.04
BID	0.18	**0.29**	**0.34**	**0.22**								0.21	0.13	0.20	-0.02
KAM	0.14	**0.36**	**0.30**	**0.22**								0.19	0.07	0.14	-0.16
BAT	0.22	**0.28**	**0.43**	**0.24**								**0.23**	0.20	0.21	-0.18
Wetnessindex (*WI*)															
TUIM	**0.27**	0.20	**0.29**	**0.27**								0.19	0.10	0.18	-0.06
SON	**0.22**	**0.30**	**0.29**	**0.33**								0.17	0.07	0.08	-0.07
BOGR	0.04	0.19	**0.36**	0.21								**0.28**	-0.03	0.09	0.02
BID	0.11	**0.30**	**0.34**	**0.25**								0.19	0.11	0.21	0.03
KAM	0.11	**0.40**	**0.31**	**0.27**								**0.27**	0.10	0.19	-0.11
BAT	0.16	**0.27**	**0.43**	**0.30**								**0.27**	0.14	**0.23**	-0.08

Correlation coefficients written in bold are significant at $p<0.05$.

* Months of the previous year.

HTC and *WI* were calculated from *Tmean* and precipitation ($HTC = 10 \cdot \sum P / \sum Tmean$, Selyaninov, 1928; $WI = 10 \cdot \log(\sum P) / \sum Tmean$, Lei et al., 2014).

Table S2. Maximum correlations of site TRW chronologies with seasonal climatic variables in the previous (*prev*) and current (*curr*) vegetative seasons

Chronology	*Tmin*	*Tmean*	*Tmax*	*P*	*SPEI*	*PDSI*	*HTC*	*WI*
prev	Jul*-Sep*			Jun*-Sep*		Sep*	Jul*-Sep*	
TUIM	-0.15	**-0.29**	**-0.36**	**0.42**	**0.43**	**0.34**	**0.40**	**0.40**
SON	**-0.23**	**-0.40**	**-0.48**	**0.53**	**0.53**	**0.41**	**0.52**	**0.49**
BOGR	-0.17	**-0.29**	**-0.35**	**0.40**	**0.38**	**0.27**	**0.35**	**0.35**
BID	-0.15	**-0.32**	**-0.40**	**0.44**	**0.46**	**0.45**	**0.45**	**0.40**
KAM	-0.21	**-0.40**	**-0.49**	**0.51**	**0.50**	**0.44**	**0.52**	**0.46**
BAT	-0.21	**-0.39**	**-0.47**	**0.52**	**0.52**	**0.43**	**0.51**	**0.48**
curr	May-Jul			Apr-Jul		May-Jul		
TUIM	-0.14	-0.21	**-0.24**	**0.37**	**0.44**	**0.49**	**0.32**	**0.28**
SON	-0.13	-0.19	**-0.22**	0.20	**0.28**	**0.41**	0.21	**0.22**
BOGR	-0.11	-0.15	-0.18	**0.28**	**0.37**	**0.41**	**0.28**	**0.26**
BID	-0.07	-0.15	-0.19	**0.36**	**0.42**	**0.55**	**0.31**	**0.23**
KAM	-0.18	**-0.27**	**-0.32**	**0.29**	**0.31**	**0.47**	**0.31**	**0.32**
BAT	-0.15	**-0.24**	**-0.26**	**0.34**	**0.43**	**0.54**	**0.34**	**0.31**
Correlation between *prev* and *curr* seasonal climatic series	**0.31**	**0.39**	**0.40**	0.11	0.14	**0.65**	**0.24**	**0.33**

Correlation coefficients written in bold are significant at $p<0.05$.

* Months of the previous year.

Note that *SPEI* is the only drought index for which here is no significant correlation between the previous and the current season series; in contrast, the *PDSI* series display very high correlation between the previous and the current season. Therefore, despite the fact that *PDSI* is better correlated with larch chronologies, *SPEI* was used as an indicator of drought in this study.

Table S3. Preliminary estimation of mean cambial ages during droughts (calculated automatically in ARSTAN without pith offset evaluation and addition, i.e., biased to the minimum values)

	Mean cambial age at the site, years				
Drought years	TUIM	SON	BOGR	BID	KAM
1951	93	33	50	61	90
1963-65	98	43	59	66	98
1974-76	102	51	70	66	104
1999	109	74	76	85	125

References

Lei, Y., Liu, Y., Song, H., Sun, B., 2014. A wetness index derived from tree-rings in the Mt. Yishan area of China since 1755 AD and its agricultural implications. Chin. Sci. Bull. 59 (27), 3449–3456. doi:10.1007/s11434-014-0410-7.

Selyaninov G.T., About climate agricultural estimation Proc. Agric. Meteorol. 1928. 165-177.